Eur Biophys J (1999) 28: 179–186

ARTICLE

Jan Domke · Wolfgang J. Parak · Michael George
Hermann E. Gaub · Manfred Radmacher

Mapping the mechanical pulse of single cardiomyocytes with the atomic force microscope

Received: 7 August 1998 / Revised version: 9 November 1998 / Accepted: 18 November 1998

Abstract The atomic force microscope (AFM) was used to analyse the contractile behaviour of embryonic chicken cardiomyocytes. The mechanical pulsing of cardiomyocytes was analysed by observing active single cells as well as cells in a confluent layer. When embedded in a confluent layer, owing to synchronisation, pulsing of the cells was often found to be very stable in terms of frequency and amplitude of the beat, including negative as well as positive amplitudes. Nevertheless, owing to movements of contraction centres within the layer, a flipping of the sign of the amplitude did sometimes also occur on a time scale of minutes. In contrast, single cells often changed between active periods of pulsing and periods of complete quietness. Also characteristic parameters like beat period and pulse amplitude were observed to be unstable. Finally, we combined the abilities of the AFM to image adherent single cells and to record locally beat amplitudes, to characterise the pulsing behaviour of single cells laterally resolved.

Key words Atomic force microscope · Chicken cardiomyocytes · Mechanical pulsing · Contraction centre

Introduction

In the last decades, cardiac myocytes have been studied in great detail, mainly by electrophysiological methods. The great interest stems from two major reasons: (1) the understanding of cardiac diseases may be improved by investigations on the cellular level and (2) owing to their ability of spontaneous generation of action potentials in vitro (Antoni 1997), they are an ideal model system to study the detailed mechanism of muscle contraction, starting from the spontaneous generation of action potentials.

The formation of action potentials has been studied extensively, usually employing microelectrodes and the patch clamp technique (Noble 1984). Up to now, the mechanical contraction behaviour of cardiomyocytes has been mainly investigated using micropipettes attached to force sensitive micromanipulators (Shepard et al. 1990). However, owing to the size of the pipettes the measured contraction force and amplitude is more like an integral number for the whole cell.

In this work, employing an atomic force microscope (AFM), we could measure the contraction amplitude locally to obtain laterally resolved maps of the mechanical beating of single cardiomyocytes.

After its invention in 1986 (Binnig et al. 1986) the AFM has emerged within only a decade to be a powerful instrument for the investigation of biological samples. Soon it was used for observing living cells under physiological conditions (Henderson et al. 1992; Radmacher et al. 1992). The high sensitivity in detecting (Florin et al. 1994) and applying (Tao et al. 1992) small forces and the high resolution in determining sample height makes the AFM an interesting tool to measure the mechanical beating of cardiomyocytes. In addition, the investigation of living cells by AFM can be done in a non-invasive manner (Schaus and Henderson 1997).

An extensive discussion of AFM application in cardiac electrophysiology has been published by Arnsdorf and Shaohua (1996). Shroff et al. (1995) used the AFM to analyse the mechanical properties of pulsing atrial myocytes, while Hofmann et al. (1997) observed the degrading effects of cytochalasin on the cytoskeleton of cardiocytes.

In the field of cardiac diseases it is of great interest to observe the lateral spreading of electrical excitement across the heart tissue. For example, the propagation direction of action potentials, i.e. parallel or perpendicular to the muscle cells, is characteristic of the electrical coupling between single muscle bundles. Age-related differences were found by analysing the extracellular poten-

J. Domke · W.J. Parak · M. George · H.E. Gaub
M. Radmacher (✉)
Lehrstuhl für Angewandte Physik,
Ludwig-Maximilians-Universität München,
Amalienstrasse 54, D-80799 München, Germany
e-mail: manfred.radmacher@physik.uni-muenchen.de

tial with microelectrodes, indicating that there is progressive electrical uncoupling of the side-to-side connections between groups of parallel-orientated atrial fibres with advancing age (Spach and Dolber 1986).

Materials and methods

Cell culture

Isolation, purification and cultivation of chicken embryo cardiomyocytes was done as described in more detail elsewhere (Riehle and Bereiter-Hahn 1994; Denyer et al. 1998; Parak et al. 1999). Briefly, hearts were extracted from 7 to 9-day-old chick embryos and enzymatically dissolved. The cell suspension was then transferred into a tissue culture flask and incubated for 1 h. This incubation allowed the majority of fibroblasts to adhere to the flask and left an increased proportion of about 80% myocytes in suspension (Blondel et al. 1971). Finally, heart cells were plated in 35 mm culture dishes (Nunc, Wiesbaden-Biebrich, Germany) at densities of about $5–10\times10^4$ cells/cm^2 and incubated for 24 h. Higher concentrations resulted in dense layers of connected cells. Every other day, the medium was exchanged. After 1–2 days in vitro, a high percentage of cells started beating.

Instrumentation

For all measurement AFM was performed with a commercial instrument (Bioscope, Digital Instruments, Santa Barbara, Calif.). To enable us to find mechanically active single cells and position the AFM tip on top of them, the AFM was placed on an inverted optical microscope (Zeiss Axiomat, Zeiss, Oberkochen, Germany). The whole AFM setup was covered by a plastic box, in which we could control and tune the atmospheric conditions to 5% CO_2 and 37 °C, i.e. to investigate the cells under environmental conditions of cell culture incubators. All experiments were performed in 35 mm culture dishes (Nunc) in cell culture medium. In this study we used silicon nitride cantilevers (Microlevers, Park Scientific, Santa Clara, Calif.), which had a force constant of about 8 mN/m calibrated with the thermal noise method (Butt and Jaschke 1995).

For recording the time series of beating heart cells we used the so-called constant force mode with the scan size set to zero. In this mode the sample height is adjusted such that the deflection stays constant employing an electronic feedback loop. The gains that drive the feedback loop controlling the deflection of the cantilever were put as high as possible without inducing the system to oscillate. Time series for pulse mapping were recorded with a loading force of about 800 pN, which was controlled via force curves before each series. In the case of the other time series, the loading force was always in the range of a few nanonewton without explicit control. However, we observed that loading forces up to 10 nN had no detectable influence on the amplitude as long as the force stayed constant during a pulse as warranted in this AFM mode.

The contact images were recorded with a slow scan rate of 0.5 Hz and 0.6 Hz, respectively, and a loading force of about 1 nN.

Parametrisation

To characterise the recorded mechanical pulses $h(t)$ of myocytes, we introduced several parameters. Pulses were analysed for the cell's total change in height, i.e. the maximum pulse amplitude, Δh, the full width at half maximum of the duration of the pulse, t_{fwhm}, and the period of pulsing, t_{p}. To characterise the geometric shape the maximum slope during depolarisation, $\mathrm{d}h_{\mathrm{dep}}/\mathrm{d}t$, and the maximum slope during repolarisation $\mathrm{d}h_{\mathrm{rep}}/\mathrm{d}t$, were calculated for each pulse. The absolute numbers of amplitude and consequently also of the slopes differed largely between individual samples and in the case of single cells even from one pulse to the next. Hence, we normalised the slope with the respective maximum amplitude Δh for each peak, yielding the so-called depolarisation time:

$$t_{\mathrm{dep}} = \frac{1}{(\mathrm{d}h_{\mathrm{dep}}/\mathrm{d}t)/\Delta h} \tag{1}$$

and repolarisation time:

$$t_{\mathrm{rep}} = \frac{1}{(\mathrm{d}h_{\mathrm{rep}}/\mathrm{d}t)/\Delta h} \tag{2}$$

De- and repolarisation time derived from the AFM recordings are related to pure mechanical effects. To compare those data with electrophysiological measurements, we introduced an additional depolarisation time, t^*_{dep}, derived from patch clamp recordings:

$$t^*_{\mathrm{dep}} = \frac{1}{(\mathrm{d}V/\mathrm{d}t)/\Delta V} \tag{3}$$

It is defined as the reciprocal normalised slope of an action potential, where $\mathrm{d}V/\mathrm{d}t$ is the maximum rate of rise and ΔV the total voltage change.

All experimental data are given as mean value ± standard deviation.

Results and discussion

The AFM principle mainly comprises a sensitive cantilever spring with the probe, i.e. the sharp AFM tip at its end. This is scanned over the sample with the help of an electronically guided piezo tube which allows lateral and vertical positioning very precisely. Particularly when investigating extremely sensitive soft samples like living cells, it is imperative to control the applied loading force of the AFM tip while scanning and thereby keeping it at a minimum to prevent the destruction of the sample. This is done electronically with the help of a feedback loop that tries to keep the cantilever deflection, i.e. the loading force, con-

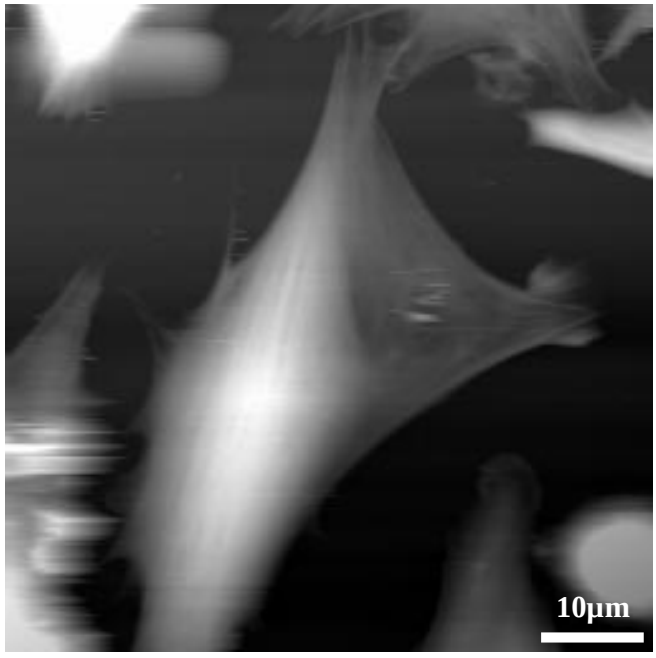

a

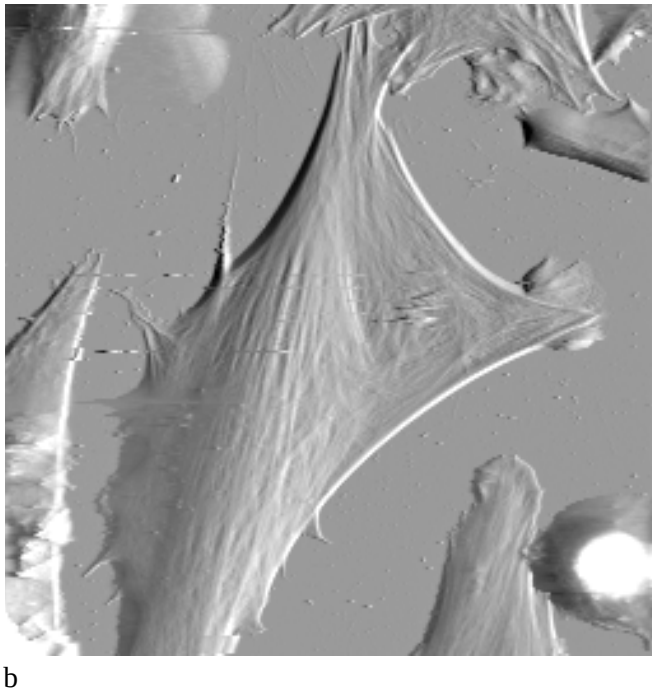

b

Fig. 1a, b Typical contact mode image of mechanically inactive cardiocytes. Particularly in the case of the height image (**a**), some poorly adherent cells caused problems while being scanned: they show an artificially large height and produce streaks that are due to bending of the cell by the scanning tip. The linear structures that are visible all over the cell in the deflection image (**b**) are due to stiff cytoskeletal structures, e.g. stress fibres, that run underneath the cell membrane

stant at a previously set value. The detected information is the height and the deflection signal, respectively. The height signal is due to the vertical movement of the piezo, and thus of the cantilever, for compensating topographical height changes. The remaining deflections due to finite response time of the feedback loop are caused by fine corrugations of the sample that cannot be compensated by the feedback loop. This so-called error signal mode is presented with the first two figures.

A typical contact mode image of living cardiocytes is shown in Fig. 1. In cell preparation the concentration of seeded cells was kept small to prevent the cells forming a confluent layer. The cells presented in Fig. 1 were mechanically inactive and did not contract during the time of investigation. As a consequence of the loading force of the AFM tip onto the cell membrane, the underlying cytoskeletal structures appear as a linear pattern, especially in the deflection signal image (Fig. 1b). These structures are visible all over the cell and presumably are stress fibers as determined in previous work (Hofmann et al. 1997). Since some of the cardiomyocytes adhered only weakly, all the rinsing and washing procedures during the change of cell medium had to be carried out very gently. Consequently, the concentration of dead or poorly adherent cells was relatively high compared to samples of adherent cell lines. Such only weakly attached cells are visible at both sides of the image, especially in the lower half. The images of these cells show prominent streaks due to bending and pushing around parts of the cells. This bending leads then also to an artificially large apparent height.

The recording of time series of cell pulsing was carried out in constant force mode by positioning the AFM tip on top of the surface of the cells. Fig. 2 shows an example of a sequence of beats recorded on a dense cell layer. It shows the height signal (Fig. 2a), where the amplitude of the pulses corresponds to the vertical expansion of the cell surface during one beat, and the deflection signal (Fig. 2b) which is caused by the finite response time of the feedback loop. The deflection signal is similar to the first derivative of the height signal which can be clearly followed in the course of the detected signals. Since the deflection signal in all measurements of time series was smaller than 6% compared to the height signal, e.g. in the case of Fig. 2 only 2%, we were always content to analyse only the height signal as it describes the characteristic features of a pulse.

Cardiomyocytes within a confluent layer of cells were observed to beat typically very regular in terms of pulse shape and frequency over long time periods. Some samples pulsed with a constant beat period with a fluctuation of less than 2% over 5 min and less than 8% over 30 min. As also described by Clay and DeHaan (1979), this stability, arising from the synchronisation between cells within the layer, was hardly ever found in samples of single cells.

Occasionally we also observed changes in the shape of the mechanical pulses in confluent layers, as will be discussed here. One example of this behaviour is shown in Fig. 3: in this stretch of data, recorded over 12 min, we observed pulses with negative amplitude (Fig. 3b) (“peak-

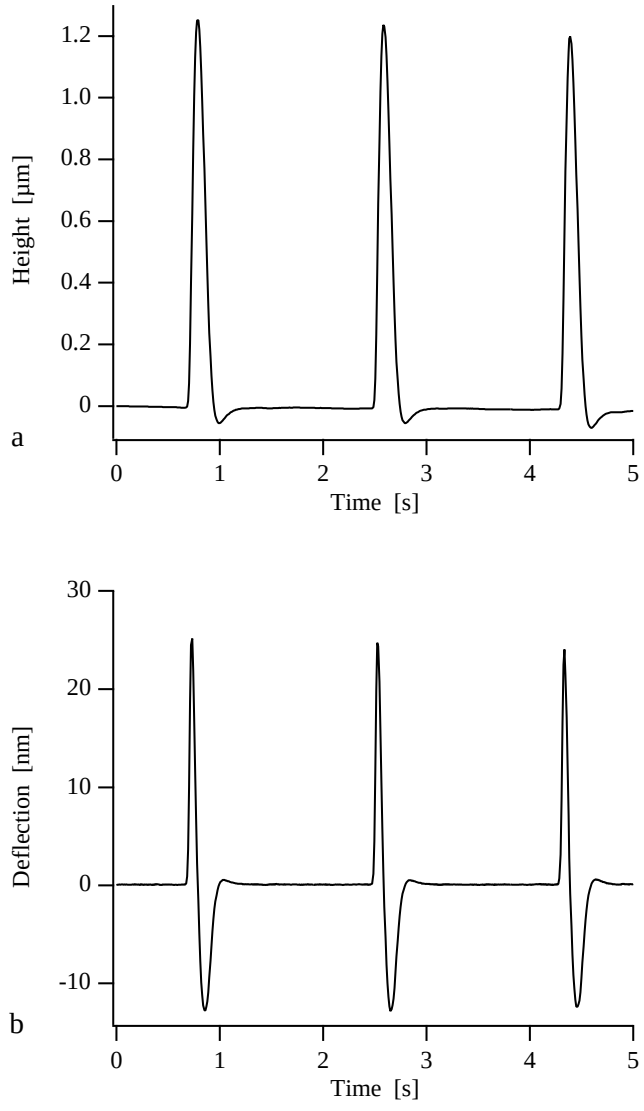

Fig. 2a, b Typical profile of mechanical beating of cardiomyocytes recorded on a confluent layer of cells. The height signal (**a**) is due to the vertical expansion of the cell as investigated with the AFM tip. In this mode of operation a feedback adjusts the cantilever height such that the deflection of the cantilever stays nominally constant. Since the feedback electronics needs finite time to compensate changes in deflection some residual variations of the deflection are observed (**b**). However, since the feedback is nearly perfect (up to 98% of height changes are corrected by it), we disregarded the deflection signal in the following discussion

down") at the beginning of the trace, which changed to a stable pattern of peaks with positive amplitude (Fig. 3f) ("peak-up") at the end of the trace. However, this transition did not occur suddenly, but over some time, where biphasic pulses were visible (Fig. 3c–e). Descriptive data for the pulse characteristics of the initial (stable peak-down) and final (stable peak-up) pulses are summarised in Table 1.

This example shows the characteristic features we typically observed with beating confluent cell layers: peaks with negative as well as positive amplitudes with a very

Table 1 Descriptive data of a 1.5 min section of the dataset of a beating layer of confluent cells before and after the flip of the amplitude. In these periods the pulses showed a behaviour of large continuity, but also within the sequence of the flipping amplitude the period of pulsing nearly stayed constant

	Beginning of measurement ("peak-down")	Sequence of flipping amplitude	End of measurement ("peak-up")
Δh	625 ± 70 nm		290 ± 65 nm
t_p	0.81 ± 0.15 s	0.87 ± 0.02 s	0.85 ± 0.03 s
t_{fwhm}	0.19 ± 0.01 s		0.24 ± 0.03 s
dh_{dep}/dt	11.0 ± 0.8 µm/s		4.1 ± 1.2 µm/s
dh_{rep}/dt	6.6 ± 1.2 µm/s		3.2 ± 0.6 µm/s
t_{dep}	57 ± 6 ms		75 ± 16 ms
t_{rep}	98 ± 16 ms		90 ± 13 ms

stable dynamics of pulsing. Here, additionally the amplitudes of the peaks flipped within roughly 2 min.

Experimental patch clamp data, which were obtained following the same cell isolation protocol as described in this study, but at room temperature, have been published recently (Parak et al. 1999). The maximum slope and the amplitude of the action potentials were found to be $dV/dt = 1.6 \pm 0.7$ V/s and $\Delta V = 67 \pm 9$ mV. Therewith the depolarisation time was calculated to be $t^*_{dep} = 42 \pm 19$ ms, which is in good agreement with the depolarisation time derived from the AFM recordings. Since the patch clamp data were recorded at room temperature, the obtained value has to be considered as an upper limit for an electrically derived depolarisation time. Indeed, with other preparation protocols much faster depolarisation times due to steeper rises of action potentials (up to 100 V/s) have been reported (Clay and DeHaan 1979; Clay et al. 1990). However, considering the manifold functional regions of the heart, this seems not to be surprising. As an example, it is well known that action potentials of cardiac pacemaker cells have quite low rates of rising (Antoni 1997).

As was visualised with the help of an optical microscope, cells in confluent layers built up macroscopical (i.e. on the millimetre scale) patterns of contraction: parts of the sample acted as centres of contraction while other (presumably more passive) cells in adjacent regions were clearly pulled laterally towards these centres during each beat. Whereas centres could be easily correlated with positive amplitudes ("peak-up"), negative amplitudes ("peak-down") were only found in regions surrounding these contraction centres. Although the period of pulsing in the dataset of Fig. 3 was stable over the whole time, the shape of the pulses suddenly started to change. Since the lateral contraction pattern of the cell layer could easily be followed in parallel by the optical microscope, this change and finally the flip in amplitude could be correlated with the movement of the centre of contraction in the near vicinity of the AFM tip.

However, it seems remarkable that on the one hand most often systems of confluent layers of cells showed an enormous stability in pulse dynamics, concerning all parameters describing the pulse shape, as well as aspects of tim-

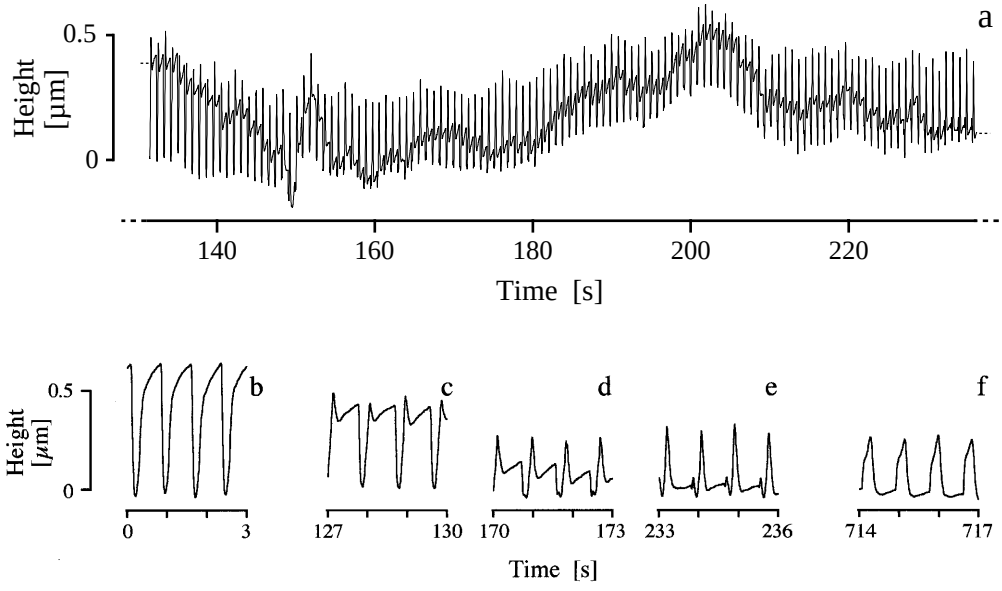

Fig. 3a–f Detail of a time series recorded on a confluent layer of pulsing cells (**a**). This sequence shows a two-fold flip in the pulse amplitude. The short sketches (**b–f**) are zooms into the dataset and present some of the characteristic pulse shapes during the flip (**c–e**). While changing the pulse shape within the observation time, the pulse period stayed nearly constant. The first (**b**) and the last (**f**) zoom-in, i.e. about 2 min before and 8 min after the flip, respectively, are characteristic pulses of the range in which a stable pulse behaviour was observed

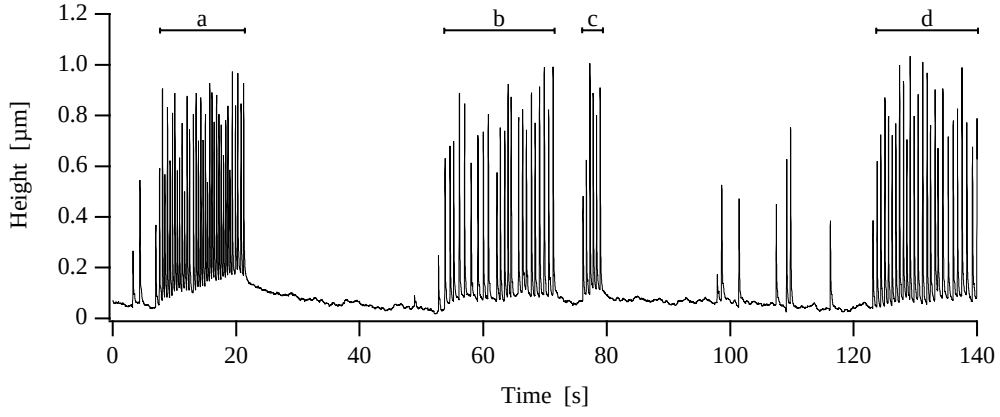

Fig. 4 Time series of the mechanical beating of a single cell. Sequences of high mechanical activity alternate irregularly with times of inactivity. While the shape of the pulses nearly stays constant, the pulse period varies within a factor of two from the first to the second active sequence. During times of passiveness, spontaneous single beats occasionally occur

ing like the periodicity. This seems to be a direct consequence of cell coupling and synchronisation at the same time. On the other hand, clearly a macroscopic behaviour of moving centres of contraction was found, which drastically influenced the local pulse characteristics in a more erratic way on a timescale of minutes.

The diverse pulse shapes like negative, positive and biphasic amplitudes or double and triple peaks (data not shown) we observed, in spite of constant beating frequencies in the case of cell layers, led us to the following question: do single cells show the same variety in their pulsing behaviour?

A typical section taken from a time series of a beating profile recorded on a single cell is shown in Fig. 4. We observed this particular cell for nearly 30 min. With the help of the optical microscope the AFM tip was positioned over the central nucleus region of this cell. Compared with the pulsing characteristic of synchronised cells within a confluent layer, two major differences to a single cell are directly visible:

1. During the time course, sequences of high mechanical activity alternated irregularly with times of quietness. Both the active and the inactive sequences often lasted for several minutes. However, single beats also occurred which interrupted quiescent times. Within the active sections the period of pulsing was somewhat regular. However, as can be seen in the statistical analysis presented in Table 2, a much higher fluctuation than in the case of synchronised cells is obvious. Moreover, the period sometimes changed drastically from one section to the other, e.g. in this example by a factor of two.
2. The pulse amplitude also showed a high fluctuation.

Thus both intervals and amplitudes of individual beats were more irregular than observed with confluent cells. Sometimes consecutive beats varied manifold in the measured height.

Since the analysed pulses had a nearly constant full width half maximum, the observed slopes consequently had a large fluctuation due to the varying amplitudes. Introducing depolarisation and repolarisation time by normalising the slopes nevertheless led to values with only small fluctuations that also stayed stable for the duration of several sequences of activity. Hence, these parameters seem to be appropriate to characterise even pulse shapes

Table 2 Statistics of the time series detail shown in Fig. 4, recorded on a single cell. To demonstrate the changes of the pulse characteristics the four marked active sequences were analysed separately. Corresponding to the respective period of time in Fig. 4, each column represents one sequence. Remarkably, only the amplitude and the period of pulsing varies on a large scale, while the other parameters characterising the pulse shape nearly stay constant

Period of time	*a* (7–21 s)	*b* (53–71 s)	*c* (76–79 s)	*d* (123–140 s)
Δh	654 ± 124 nm	714 ± 107 nm	687 ± 184 nm	770 ± 127 nm
t_p	0.41 ± 0.06 s	0.80 ± 0.23 s	0.55 ± 0.03 s	0.67 ± 0.11 s
t_{fwhm}	75 ± 3 ms	77 ± 4 ms	78 ± 2 ms	77 ± 3 ms
dh_{dep}/dt	20.0 ± 3.7 μm/s	20.7 ± 3.1 μm/s	20.3 ± 5.2 μm/s	22.8 ± 3.7 μm/s
dh_{rep}/dt	10.9 ± 1.5 μm/s	10.7 ± 1.5 μm/s	10.1 ± 2.8 μm/s	11.7 ± 2.1 μm/s
t_{dep}	34 ± 2 ms	34 ± 2 ms	34 ± 1 ms	33 ± 1 ms
t_{rep}	66 ± 4 ms	67 ± 3 ms	68 ± 4 ms	66 ± 4 ms

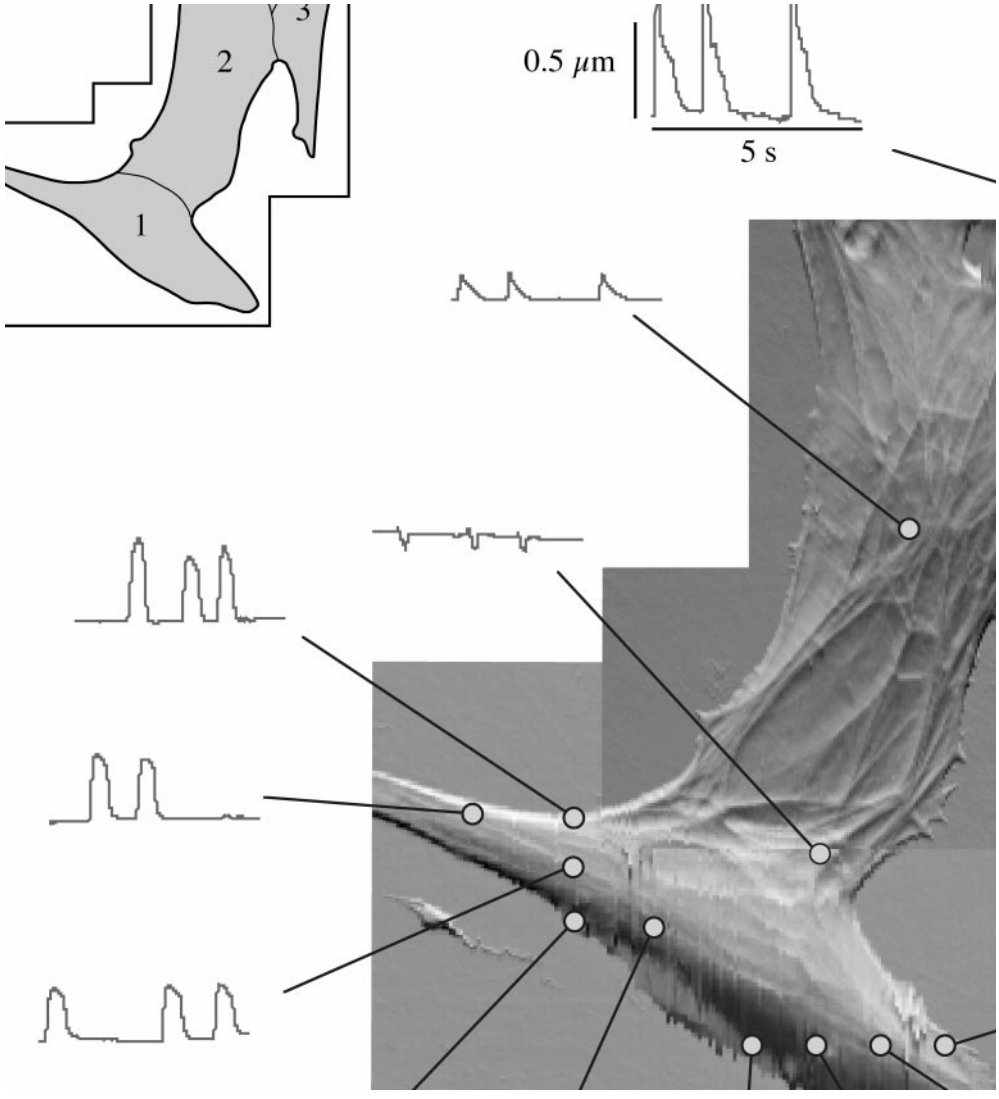

Fig. 5 Pulse mapping on a group of active cardiomyocytes. Although these cells were mechanically pulsing, it was possible to image them. In this figure the deflection images of two scans were superimposed. The cell margins are sketched in the inset on the left top. Several time series at different locations on the cells were recorded. The presented sequences are scaled identically; their locations on top of the cells are marked with circular spots. Remarkably, from all the taken series on the four cells no pulses were found that showed negative amplitude. Only the series between cells nos. 1 and 2 showed a biphasic pulse shape

of irregularly beating single cells. Although the pulse amplitude varied often up to a factor of two and the pulse period often changed in an erratic way, predominantly from one active sequence to the next, the normalised parameters stayed stable with only a small drift and hence showed the same behaviour as observed in a layer of cells.

Finally, we wanted to characterise the pulsing of a single cell in a laterally resolved manner. The basic idea was, that during the contraction of a myocyte, the volume of the cell should stay constant. Following this consideration and taking into account the observation of positive amplitudes, i.e. a lifting-up of the upper membrane at some parts of the cell, we also expected some parts to show negative ampli-

Table 3 Statistics of the time series recorded for the pulse mapping shown in Fig. 5. *n* is the number of time series that were recorded on the respective cell. For cells nos. 1 and 3 the given fluctuation is the standard deviation among the time series, in case of cells nos. 2 and 4 it is the standard deviation within the analysed pulses. With a comparatively small fluctuation, the values of t_{fwhm} and t_{dep} seem to be especially characteristic for respective cells

	Cell no. 1	Cell no. 2	Cell no. 3	Cell no. 4
n	11	1	4	1
Δh	290 ± 134 nm	134 ± 36 nm	683 ± 337 nm	408 ± 45 nm
t_{fwhm}	406 ± 24 ms	338 ± 61 ms	191 ± 55 ms	303 ± 40 ms
t_{dep}	75 ± 12 ms	49 ± 4 ms	37 ± 4 ms	74 ± 16 ms
t_{rep}	120 ± 13 ms	206 ± 45 ms	126 ± 49 ms	161 ± 37 ms

tudes, i.e. a falling-off of the upper membrane, as was observed in the case of a confluent layer. The major problem in the execution of this part of the study was the adhesion behaviour of the cells. Since it was necessary to scan individual beating single cells, the respective cells had to be attached well to the substrate. However, most of the beating single cells were only loosely attached, possibly only at a single region of adhesion. Therefore, imaging of active single cells without bending and pushing around the cell was a rarity.

A deflection image of a group of beating cardiomyocytes is shown in Fig. 5, which is a superposition of two separate images. The inset on the left top shows schematically the outline of the cells. To make the discussion easier we also numbered the cells. Despite their mechanical activity, at least the cells nos. 1 and 2 were sufficiently adherent to the substrate to allow us imaging. The two cells on the right top (nos. 3 and 4) were too high for the limited *z*-scan range of the AFM piezo. As estimated through the optical microscope, these two cells had a length of about 200 µm and had a distinct elongated spindle-like shape. The pulses of the four cells were synchronised, as observed optically. Since the cells were pulsing during the scanning procedure, the image shows many streaks that appear as a consequence of the moving cell surface. Besides imaging, we also recorded time series of the pulsing of the cells at different locations, especially on the surface of cell no. 1. The loading force during the time series was kept constant at 800 pN, which was controlled via force curves before each measurement.

As shown in Fig. 5, all the observed pulses had a positive ("peak-up") amplitude. Also in other experiments we were not able to detect negative pulses, except biphasic pulses, e.g. at the border between cells nos. 1 and 2. Since this region clearly showed distinct cytoskeletal structures, it seems plausible that in this case the biphasic pulses arise from the lateral movement of presumably stress fibres underneath the AFM tip. The statistical analysis of these time series except the biphasic pulses is presented in Table 3.

The pulse characteristics of cell no. 2 merits discussion: the observed pulses differ from those recorded on the other cells by exhibiting a small amplitude and a remarkable flat slope, i.e. a long repolarisation time t_{rep}. Also the cytoskeleton has a more net-like than linear structure. Finally, the cell is spread well and despite a larger surface area its height is about 80% of that of cell no. 1. These differences may be explained by the following hypothesis: the preparation procedure accumulates cardiomyocytes only up to a concentration of about 80% (Blondel et al. 1971). This means that there are also other cell types like cardiac fibroblasts within the preparation. Therefore it seems plausible that the mentioned peculiarities arise from the fact that cell no. 2 either is not a cardiomyocyte or is inactive. The cell itself then would have acted as kind of a transmitter, which coupled the synchronisation of cell no. 1 and cells nos. 3 and 4. The different pulse shape then might be explained with a merely passive pulsing motion that was caused more likely by the mechanical contact to the active adjacent cells than by its own active contraction.

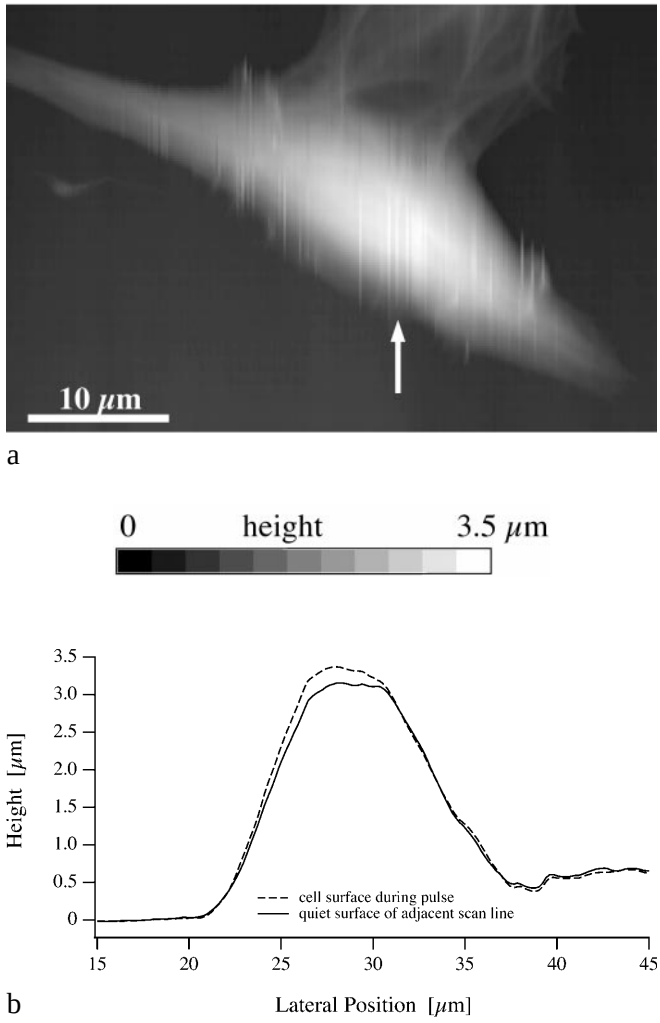

Fig. 6 **a** Height image of cell no. 1. As a consequence of the elevation of the cell's upper surface during pulsing, the image shows many streaks. The location of the profile of the cell's surface from two adjacent scan lines (**b**) is marked with an *arrow*. The first trace was recorded while the cell was relaxed, whereas the second trace (*dashed line*) coincided with a pulse of the cell. The elevation of the surface of the cell was about 280 nm maximum, which is in good agreement with the amplitudes observed in the time series of Fig. 5

The height image of cell no. 1 is shown in Fig. 6a. As mentioned already in connection with Fig. 5, the streaks in the contact image are due to the mechanical beating of the cell. In the case of cell no. 1 the duration of a pulse was longer than the time needed for crossing the cell during a single scan line. Hence, we obtained traces of the cell while being excited and while being relaxed. By comparing adjacent traces, we could relate the shape of the excited and the relaxed cell. However, since scanning and beating were not synchronised, this comparison has to be regarded cautiously. In Fig. 6b we superimposed the profiles of two adjacent scan lines: one shows the expanded excited status, the other the relaxed status before and after the pulse, respectively. The scan direction was from left to right, i.e. following increasing x-values. In Fig. 6a we marked the location of these traces across the central region of the cell with an arrow. The observed difference between the relaxed trace and the adjacent excited one gives a maximum expansion amplitude Δh of 280 nm, which is in good agreement with the data of the time series, shown in Fig. 5.

Conclusions

We investigated the pulse behaviour of chick cardiomyocytes and compared the characteristics of single cells with those of cells that were embedded in a confluent layer. We found significant differences in the stability of the pulse frequency. However, the shape of the pulses, in particular their width and the time of depolarisation, varied markedly between individual cells. Typical values were in the range of 60–410 ms for the full width at half maximum (t_{fwhm}) and 25–80 ms for the depolarisation time (t_{dep}). Since temporal fluctuations of these parameters for the same cell were very small, they seem to be characteristic parameters for each individual cell.

To our knowledge, we are the first to have investigated the mechanical pulsing of a single cell as a function of the lateral position on the cell. As result, the parameters characterizing the pulse shape were nearly similar and independent of position.

Acknowledgements This work was supported by the Deutsche Forschungsgemeinschaft as part of the "Schwerpunkt für neue Techniken in Biologie und Medizin" (J. D., M. R.) and by BMBF Germany, grant no. 0310845A (W. J. P., M. G., H. E. G.).

References

Antoni H (1997) Erregungsphysiologie des Herzens. In: Schmidt RF, Thews G (eds) Physiologie des Menschen. Springer, Berlin Heidelberg NewYork, pp 472–497

Arnsdorf MF, Shaohua X (1996) Atomic (scanning) force microscopy in cardiovascular research. J Cardiovasc Electrophys 7: 639–652

Binnig G, Quate CF, Gerber C (1986) Atomic force microscope. Phys Rev Lett 56: 930–933

Blondel B, Roijen I, Cheneval JP (1971) Heart cells in culture: a simple method for increasing the proportion of myoblasts. Experientia 27: 356–358

Butt H-J, Jaschke M (1995) Thermal noise in atomic force microscopy. Nanotechnology 6: 1–7

Clay JR, DeHaan RL (1979) Fluctuations in interbeat interval in rhythmic heart-cell clusters. Biophys J 28: 377–389

Clay JR, Brochu RM, Shrier A (1990) Phase resetting of embryonic chick atrial heart cell aggregates. Biophys J 58: 609–621

Denyer MCT, Riehle M, Britland ST, Offenhäuser A (1998) A preliminary study on the suitability of a pharmacological bioassay based on cardiac myocytes cultured over microfabricated microelectrode arrays. Med Biol Eng Comput 36 (in press)

Florin E-L, Moy VT, Gaub HE (1994) Adhesion forces between individual ligand-receptor pairs. Science 264: 415–417

Henderson E, Haydon PG, Sakaguchi DS (1992) Actin filament dynamics in living glial cells imaged by atomic force microscopy. Science 257: 1944–1946

Hofmann UG, Rotsch C, Parak WJ, Radmacher M (1997) Investigating the cytoskeleton of chicken cardiocytes with the atomic force microscope. J Struct Biol 119: 84–91

Noble D (1984) The surprising heart: a review of recent progress in cardiac electrophysiology. J Physiol (Lond) 353: 1–50

Parak WJ, Domke J, George M, Kardinal A, Radmacher M, Gaub HE, deRoos ADG, Theuvenet APR, Wiegand G, Sackmann E, Behrends JC (1999) Electrically excitable NRK fibroblasts – a new model system for cell-semiconductor hybrids. Biophys J 76 (in press)

Radmacher M, Tillmann RW, Fritz M, Gaub HE (1992) From molecules to cells – imaging soft samples with the AFM. Science 257: 1900–1905

Riehle M, Bereiter-Hahn J (1994) Ouabain and digitoxin as modulators of chick embryo cardiomyocyte energy metabolism. Arzneimittelforschung 44: 943–947

Schaus SS, Henderson ER (1997) Cell viability and probe-cell membrane interactions of XR1 glial cells imaged by atomic force microscopy. Biophys J 73: 1205–1214

Shepard N, Vornanen M, Isenberg G (1990) Force measurements from voltage-clamped guinea pig ventricular myocytes. Am J Physiol 258: H452–H459

Shroff SG, Saner DS, Lal R (1995) Dynamic micromechanical properties of cultured rat atrial myocytes measured by atomic force microscopy. Am J Physiol 269: C286–C292

Spach MS, Dolber PC (1986) Relating extracellular potentials and their derivatives to anisotropic propagation at a microscopic level in human cardiac muscle. Circ Res 58: 356–371

Tao NJ, Lindsay NM, Lees S (1992) Measuring the microelastic properties of biological material. Biophys J 63: 1165–1169